

## Enzymes

How to cite: *Angew. Chem. Int. Ed.* **2022**, *61*, e202210883

International Edition: doi.org/10.1002/anie.202210883

German Edition: doi.org/10.1002/ange.202210883

# Sactipeptide Engineering by Probing the Substrate Tolerance of a Thioether-Bond-Forming Sactisynthase

Ataurehman Ali, Dominic Happel, Jan Habermann, Katrin Schoenfeld,  
 Arturo Macarrón Palacios, Sebastian Bitsch, Simon Englert, Hendrik Schneider,  
 Olga Avrutina, Sebastian Fabritz, and Harald Kolmar\*

In memory of Ulf Diederichsen.

**Abstract:** Sactipeptides are ribosomally synthesized peptides containing a unique sulfur to  $\alpha$ -carbon cross-link. Catalyzed by sactisynthases, this thioether pattern endows sactipeptides with enhanced structural, thermal, and proteolytic stability, which makes them attractive scaffolds for the development of novel biotherapeutics. Herein, we report the in-depth study on the substrate tolerance of the sactisynthase AlbA to catalyze the formation of thioether bridges in sactipeptides. We identified a possible modification site within the sactipeptide subtilisin A allowing for peptide engineering without compromising formation of thioether bridges. A panel of natural and hybrid sactipeptides was produced to study the AlbA-mediated formation of thioether bridges, which were identified mass-spectrometrically. In a proof-of-principle study, we re-engineered subtilisin A to a thioether-bridged, specific streptavidin targeting peptide, opening the door for the functional engineering of sactipeptides.

## Introduction

Within recent decades, numerous natural and synthetic miniproteins—characteristically folded oligopeptides possessing a stabilizing pattern usually based on covalently linked side chains of cysteines—came into the focus of biomedical and biotechnological applications due to their unique structural features and excellent tunability.<sup>[1]</sup> Various reports have shown that these architectures can be endowed with novel properties by simple loop grafting, thus enormously broadening their application spectrum, from molecular modelling to medicine.<sup>[1b,2]</sup> Recently, certain miniproteins were reported to bind the spike receptor binding domain (RBD) of SARS-CoV-2, thus inhibiting infection.<sup>[3]</sup> These inhibitory miniproteins had binding affinities ranging from high picomolar to low nanomolar, demonstrating the high potential of this peptide class for medical applications.<sup>[3]</sup> Within the huge family of miniproteins, sactipeptides represent a unique group due to their distinctive 3D architecture and side chain bridging, rare occurrence (only ten members have been described to date) and promising bioactivities. Indeed, these ribosomally synthesized and post-translationally modified peptides (RiPPs) possess a really uncommon motif in biomolecules that comprises at least one linkage between a cysteine side chain thiol and the  $\alpha$ -carbon of a certain residue other than Cys (Thr, Ala, Phe, etc.). Such a residue is referred to as an acceptor amino acid (Figure 1A). Only a few representatives of this family were studied in detail, among them subtilisin A, sporulation killing factor, thurincin H, the two-component thurincin CD, thurincin Z/Huazacin, streptosactin, Hyicin 4244, ruminococcin C1, and the recently identified QmpA (Figure 1B).<sup>[4]</sup> Generally, sactipeptides can be divided into two types: Type I, made up of a nested hairpin with the cysteines and the acceptor amino acids located *N*- and *C*-terminally, respectively, and Type II defined by an unnested hairpin (Figure 1B).<sup>[5]</sup> Like all RiPPs, sactipeptides are synthesized as precursor peptides with an *N*-terminal leader peptide and a *C*-terminal core peptide. The leader peptide is recognized by radical S-adenosylmethionine (rSAM) enzymes containing at least two [4Fe-4S] clusters which mediate the introduction of thioether crosslinks into the core peptide (Figure 1A).<sup>[6]</sup> These so-called sactisynthases, which belong to the subtilisin/PQQ/anaerobic sulfatase maturing en-

[\*] Dr. A. Ali, D. Happel, J. Habermann, K. Schoenfeld,  
 Dr. A. Macarrón Palacios, S. Bitsch, S. Englert, Dr. H. Schneider,  
 Dr. O. Avrutina, Prof. Dr. H. Kolmar  
 Department for Organic Chemistry and Biochemistry, Technische  
 Universität Darmstadt,  
 Alarich-Weiß-Straße 4, 64287 Darmstadt (Germany)  
 E-mail: Harald.Kolmar@TU-Darmstadt.de

Dr. S. Fabritz  
 Department of Chemical Biology, Max Planck Institute for Medical  
 Research  
 Jahnstraße 29, 69120 Heidelberg (Germany)

Prof. Dr. H. Kolmar  
 Centre for Synthetic Biology, Technical University of Darmstadt  
 64283 Darmstadt (Germany)

© 2022 The Authors. Angewandte Chemie International Edition published by Wiley-VCH GmbH. This is an open access article under the terms of the Creative Commons Attribution Non-Commercial License, which permits use, distribution and reproduction in any medium, provided the original work is properly cited and is not used for commercial purposes.

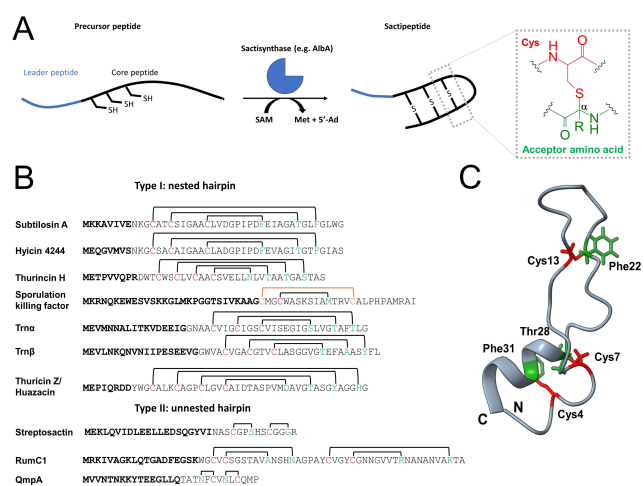


**Figure 1.** Overview of sactipeptide synthesis, sequences and structural hallmarks. A) Modification of sactipeptide precursors by the respective sactisynthases, through radical cleavage of the co-substrate S-adenosylmethionine to methionine and a 5'-deoxyadenosyl radical. Chemical structure of a thioether bridge shown in grey dotted box. B) Sequences of identified Type I and Type II sactipeptides. Thioether linkages are indicated with a black line, disulfide connections are shown in orange. The respective leader peptides are shown in bold. C) Crystal structure of sboA. Cysteines and the corresponding acceptor amino acids involved in a thioether cross-linkage are shown in red and green, respectively. Crystal structure PDB: 1PXQ. Illustration was generated with ChimeraX.

zyme (SPASM) family, directly catalyze the hydrogen abstraction of the  $\alpha$ -carbon from the acceptor amino acid, leading to a ketoimine intermediate which is then nucleophilically attacked by the corresponding cysteine thiol.<sup>[4h,6,7]</sup> During the post-translational maturation, the leader sequence is eventually cleaved. Further enzymatic modifications such as for example *N*-to *C*-terminal cyclization yield the mature sactipeptide.

Some sactipeptides exhibit a narrow antibiotic activity against drug-resistant human pathogenic bacteria, which may become particularly important in the future considering that the world is on the verge of a major antibiotic crisis.<sup>[4e,k,8]</sup> Their heat and proteolysis resistance due to thioether crosslinks and the unique and stable hairpin structure (Figure 1C) render sactipeptides as attractive scaffolds for biotechnological applications.<sup>[4a,h,i,8,9]</sup> In particular, the exposed loop between Cys13–Phe22 of the sactipeptide subtilosin A (sboA) might become attractive for bioengineering (Figure 1C) if one succeeds in the insertion of novel target binding peptide sequences without compromising enzyme-mediated thioether bridge formation. Previous research on the substrate promiscuity of sactio-nine-catalyzing AlbA revealed that changes in the loop (Cys13–Phe22) and at the *C*-terminal part of the peptide are tolerated.<sup>[4h,10]</sup> These results indicate that sboA is a promising scaffold for the introduction of novel functionalities as it has been shown for lanthipeptides which contain thioether bonds between Cys and Ser/Thr side chains and other miniproteins that display a disulfide-bridged cystine knot architecture.<sup>[1b,2a,11]</sup>

In an effort to introduce a novel bioactivity into sboA, it was required to assess the substrate promiscuity of AlbA, the enzyme that catalyzes the formation of the mentioned characteristic thioether motif, particularly in view of the fact that chemical routes for the total synthesis of sactipeptides are currently lacking. For a better understanding of AlbA substrate tolerance, we studied the formation of thioether-containing peptides by endowing various sactipeptides with the sboA leader peptide. We also generated hybrid peptides comprising the *N*-terminal part of sboA and the *C*-terminal part of other Type I sactipeptides to broaden the knowledge about AlbA substrate tolerance and also to understand the effects of relative positional shifts of the residues involved in thioether bond formation. Finally, we investigated the enzyme performance upon the introduction and/or substitution of amino acid sequences possessing different numbers of residues to investigate a potential loop grafting strategy.

## Results and Discussion

### Elongation of sactipeptides by the sboA leader peptide

Having considered the work of Flöhe et al., Himes et al., and Burkhart et al., who laid the groundwork for analyzing the substrate tolerance of AlbA, we further investigated in more detail the substrate promiscuity of AlbA.<sup>[4h,7c,12]</sup> All sactipeptides known to date possess different leader sequences which serve as recognition sites and landing points for the respective sactisynthase.<sup>[7c]</sup> To investigate this in more detail, the leader peptide of sboA was genetically fused to the *N*-terminus of four Type I (Hyicin 4244, Trn $\alpha$ , Trn $\beta$  and Huazacin) and one Type II (Streptosactin) sactipeptides, while maintaining their original leader sequence (Figure 2A) to investigate, whether these peptides that share a common sboA leader peptide are processed by AlbA. A similar approach in which the leader peptide of a thiazoline introducing enzyme was placed upstream of the complete sboA sequence has been recently reported to generate a sboA variant carrying two thioethers and thiazolines, respectively.<sup>[12]</sup>

All constructs were produced in presence of AlbA as fusion with a *C*-terminal thioredoxin (Trx) under semi-anaerobic conditions (Figure S1). Some RiPPs are known to be quite hydrophobic and “sticky” and synthesis as Trx fusion was found to be crucial to provide good solubility, eventually leading to acceptable expression yields. Not unexpected, some sactipeptide constructs upon proteolytic removal of the Trx moiety displayed stickiness to hydrophobic surfaces and therefore were obtained in low yield. Iodoacetamide (IAA) treatment was performed under reducing conditions to carboxymethylate free cysteine thiols (Figure S2). The formation of a thioether bridge results in a net loss of two hydrogens, correlating to a loss of 2 Da, which can be difficult to differentiate between multiple modification states of the peptide. Therefore, the labelling of unreacted Cys residues with IAA can ease the distinction between the different modification states of the peptide, as it leads to a shift of 57.07 Da in the mass spectrum.<sup>[4j,7c,13]</sup>

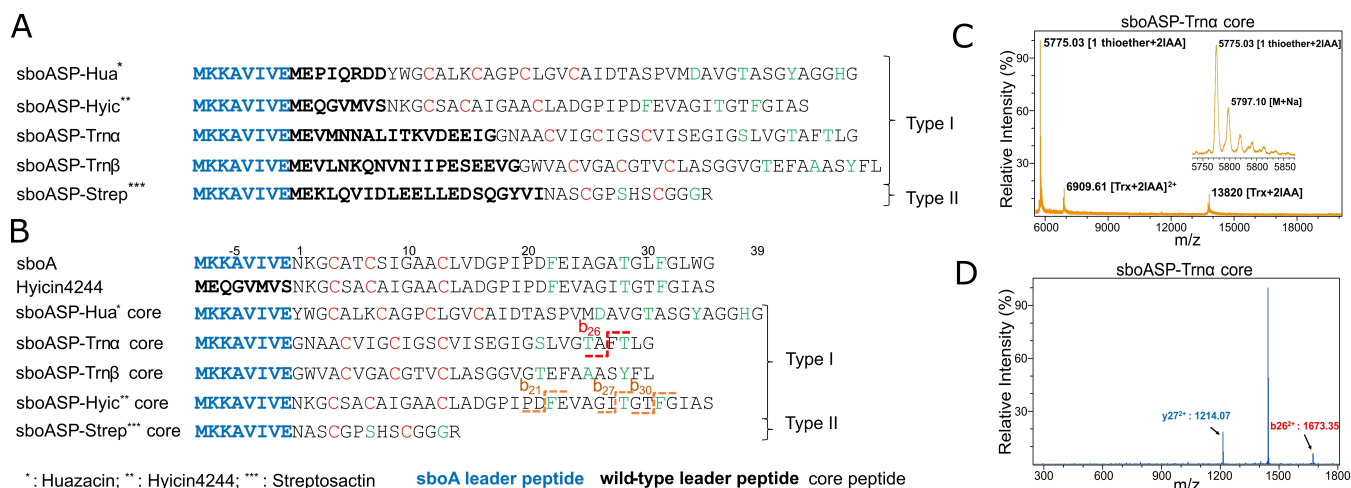


**Figure 2.** Probing leader sequence recognition by AlbA. A) Fusion of the *sboA* leader peptide to the N-terminus of various known sactipeptides. The respective leader peptide is shown in bold letters, the *sboA* leader is colored blue. B) Substitution of the natural leader peptide in sactipeptides by the *sboA* leader. Cys residues and the corresponding acceptor amino acids involved in a thioether cross link in the respective wildtype peptides are indicated in red and green, respectively. Identified acceptor position for *sboASP-Trna core* visualized with a red dotted line. Identified acceptor positions for the single thioether crosslink in *sboASP-Hyc core* shown in an orange dotted line. C) MALDI of *sboASP-Trna core* showing the introduction of one thioether crosslink. A small fraction of twice labelled thioredoxin (with IAA) is also detected (Trx: 13706 Da + 114 Da [2 labelled Cys]). The mass 6909.61 depicts the two times positive charged mass of twice labelled Trx. D) MS/MS result of *sboASP-Trna core* with the respective y and b fragments.

Finally, Trx was cleaved off applying TEV protease digestion, and the samples were analyzed with MALDI- and ESI-TOF to identify thioether bridges. Unfortunately, the constructs *sboASP-Trna* and *sboASP-Trnβ* were successfully purified as Trx fusion but could not be detected by MALDI, neither with nor without Trx (data not shown). In general, in our hands AlbA was not able to introduce thioether crosslinks into sactipeptide precursors that were elongated by the *sboA* leader sequence (Table 1, Figure S3). Although this outcome was expected for the Type II peptide Streptosactin due to its distinct architecture, in case of Hycin 4244 we anticipated that AlbA would be able to introduce at least one thioether bridge into the core peptide, since Hycin 4244 shows high homology to *sboA* (Figure S8).<sup>[4e]</sup> It might be possible that AlbA or sactisynthases in general cannot introduce a modification into the core peptide in case their respective leader sequences are placed too far away from the modification sites.

### Substitution of leader peptides by the *sboA* leader

To investigate AlbA substrate tolerance in more detail, we replaced the respective leader sequences of various sactipeptides by that of *sboA*, thereby placing the *sboA* leader directly in front of the respective core sequence (Figure 2B). With this setting, two constructs, namely *sboASP-Trna core* and *sboASP-Hyc core* were partially modified by AlbA (Figure 2B–D, Figure S4). *SboASP-Trna core* contained one thioether crosslink and two labelled cysteine residues, while wildtype Trna possesses three thioether modifications (Figure 2C). Through MS/MS analysis we identified the acceptor position to be F27 (Figure 2B & D, Figure S5). Identification

of acceptor positions applying MS/MS, is a well-established and in literature described procedure. The thioaminals of the characteristic thioether bridges are reported to undergo a retro-elimination and tautomerization process forming a dehydro-amino acid. Due to its instability compared to a normal peptide bond, this newly formed amide located at the acceptor residue is cleaved at low collision voltages, which allows the exact localization of the acceptor residue (Figure S6).<sup>[4h,5a,14]</sup> The mechanism of thioamide bond breakage has been recently re-evaluated.<sup>[15]</sup> During MS/MS analysis, fragment ion signals were validated based on charge state, mass accuracy and isotopic pattern matching (measured isotopic pattern vs. theoretical pattern). The identification of acceptor position F27 was rather surprising, as in wildtype Trna the acceptor amino acids are T25 and T28 for the second and third thioether bridge, respectively (for sequence comparison see Figure S7).

While after TEV cleavage *sboASP-Trnβ core* was not revealed by MALDI analysis (data not shown), *sboASP-Hyc core* also showed AlbA-mediated thioether bridge formation, albeit with strongly reduced efficiency, since mainly a species with one thioether bridge together with minor quantities of variants with two and three bridges were detected (Figure S4). Hycin 4244 shows high sequence identity to *sboA* (for sequence alignment see Figure S8) which indicates that already small changes in the core sequence and structure have an impact on AlbA mediated bridging.<sup>[4e]</sup> Of particular note, MS/MS analysis of *sboASP-Hyc core* revealed that all three proposed acceptor residues of the Hycin 4244 core peptide were addressed individually by AlbA to form the thioether crosslink (Figure S8 & S9). This result suggested that although AlbA recognized the three possible acceptors individually in Hycin 4244 (Fig-

**Table 1:** Summary of all generated constructs. Orange: identified acceptor positions for the single thioether bridge.

|                                    | Construct                               | Thioether  | Acceptor amino acid position |
|------------------------------------|---|------------|------------------------------|
| <b>Leader peptide addition</b>     | <i>sboASP-Hua</i> <sup>[a]</sup>        | 0          | –                            |
|                                    | <i>sboASP-Hyic</i> <sup>[b]</sup>       | 0          | –                            |
|                                    | <i>sboASP-Trnα</i>                      | No product | –                            |
|                                    | <i>sboASP-Trnβ</i>                      | No product | –                            |
|                                    | <i>sboASP-Strep</i> <sup>[c]</sup>      | 0          | –                            |
| <b>Leader peptide substitution</b> | <i>sboASP-Hua</i> <sup>[a]</sup> core   | 0          | –                            |
|                                    | <i>sboASP-Hyic</i> <sup>[b]</sup> core  | 1          | a1, a7, a10                  |
|                                    | <i>sboASP-Trnα</i> core                 | 1          | a7                           |
|                                    | <i>sboASP-Trnβ</i> core                 | No product | –                            |
|                                    | <i>sboASP-Strep</i> <sup>[c]</sup> core | 0          | –                            |
| <b>Hybrid peptides</b>             | <i>sboAD22Hua</i>                       | 0          | –                            |
|                                    | <i>sboAF22Hyic</i> <sup>[b]</sup>       | 3          | a1, a7, a10                  |
|                                    | <i>sboASP-HyicL13sboA</i>               | 0          | –                            |
|                                    | <i>sboAS22Trnα</i>                      | 1          | a7                           |
|                                    | <i>sboAS22FTrnα</i>                     | 1          | a7                           |
|                                    | <i>sboAT22Trnβ</i>                      | 1          | –                            |
| <b>Loop insertions</b>             | <i>sboARG3</i>                          | 3          | a1, a7, a10                  |
|                                    | <i>sboARGD9</i>                         | 3          | a1, a7, a10                  |
|                                    | <i>sboAsfI1</i>                         | 0          | –                            |
|                                    | <i>sboAsfI3</i>                         | 0          | –                            |
|                                    | <i>sboAsfI5</i>                         | 0, 1, 3    | –                            |
|                                    | <i>sboAsfI9</i>                         | 3          | a1, a7, a10                  |
|                                    | <i>sboAαS8</i>                          | 2          | a7, a10                      |
|                                    | <i>sboAαS8</i> <sup>C13A</sup>          | 2          | a7, a10                      |
|                                    | <i>sboAsII</i>                          | 3          | n. D.                        |

[a] Huazacin; [b] Hyicin 4244; [c] Streptosactin; n.D.: not determined

ure S8), the overall sequence alterations impaired its concurrent access to all three acceptor residues. As for the variants containing their own leader peptide sequence, *sboASP-Hua* core and *sboASP-Strep* core did not reveal any thioether formation (Figure S4). Interestingly, the successful modification of Trnα and Hyicin 4244 core peptides, albeit only one thioether crosslink was introduced, revealed the limited ability of AlbA to accept non-native sactipeptides when the corresponding leader peptide preceded the native peptide sequence. To our knowledge, this is the first reported case, where a sactisynthase modified a sactipeptide of a different gene cluster.

### Generation of *sboA* hybrid peptides

Next, since we observed that AlbA introduced a thioether connection in the Trnα core on F27 instead of T25 or T28, we were interested to investigate whether AlbA has designated positions to introduce thioether linkages into its substrates.

Therefore, we exchanged the C-terminal sequence of *sboA* (directly after the loop) with the counterpart of other Type I sactipeptides, to generate *sboA* hybrid peptides (Figure 3A & B). Two hybrid peptides, namely those containing the Hyicin 4244 and the Trnα C-terminal fragment, respectively, showed thioether crosslinks (Figure 3C, Table 1, Figure S10–S12). In *sboAF22Hyic*, all three thio-

ether bridges were formed and the distinctive MS/MS pattern confirmed the crosslinks at the same positions as in parent *sboA* and the proposed sites in Hyicin 4244: F22, T28 and F31 (Figure 3B & C, Figure S11).<sup>[4g]</sup> Hyicin 4244 is a novel, still uncharacterized sactipeptide discovered in *Staphylococcus hyicus 4244*, that shows high sequence identity to the characterized *sboA*.<sup>[4g]</sup> For this peptide, Duarte et al. hypothesized the same connectivity as in *sboA*.<sup>[4g]</sup> With high probability, Hyicin 4244 will have the same acceptor positions when modified by its natural sactisynthase. To analyze the influence of the N-terminal part of the core peptide on AlbA-mediated thioether formation we produced a hybrid construct which consisted of the N-terminal domain of Hyicin 4244 (AA 1–13) and the C-terminal part of *sboA* (AA 13–35) (Figure 3B). This hybrid peptide revealed no modification, further underlining the importance of a conserved N-terminal peptide region for recognition by AlbA (Figure S10).

One thioether bridge was formed in *sboAS22Trnα* at F28 with approximately 60% yield (Figure S12). Interestingly, this connection was introduced at the same position as in *sboASP-Trnα* core which contains the full-length sequence of mature Trnα (F27, Figure 2B, Figure S5). This coincidence is schematically outlined in Figure S7. Notably, when replacing serine by phenylalanine which is found in subtilosin A at this position (*sboAS22FTrnα*, Figure S7) no additional thioether bridge was observed but F28 showed nearly full conversion (Figure 3C).<sup>[4h]</sup> The distance of the

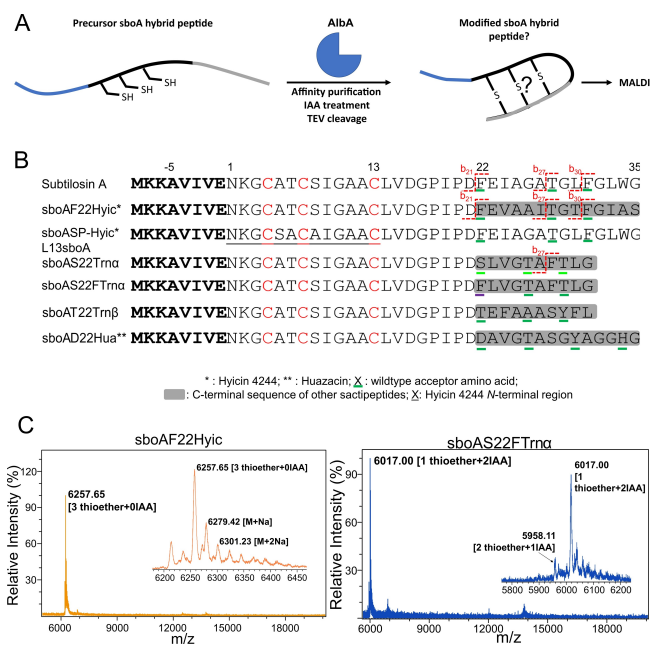


**Figure 3.** Generation of *sboA* hybrid peptides. A) General strategy of *sboA* hybrid peptide formation. *blue*: *sboA* leader peptide, *black*: *N*-terminal part of *sboA*, *grey*: *C*-terminal part of other sactipeptides. B) Generated *sboA* hybrid peptide constructs. Residues identified as acceptor positions are marked with a dotted red line alongside the resulting b fragments. Wildtype acceptor positions of the respective peptides are indicated with a green line. Purple line indicates the S22F mutation site. C) Resulting MALDI spectra shown exemplarily for two constructs. *SboAF22Hyc* shows a homogeneous product with three thioether bridges. *SboAS22FTrna* shows a product with one formed crosslink.

The residue modified by AlbA from the loop region is the same for the *sboA*-Trna hybrid peptide compared to wildtype *sboA* (Figure S7). Hence, it is tempting to speculate that both the local sequence environment and preformation of secondary structure of the sactipeptide plays a role in the post-translational modification.

### Functionalization of *sboA* by loop grafting

Further, the tolerance of AlbA to replacements and amino acid insertions into the loop of *sboA* between Cys13–Phe22 was probed. For a better understanding, we divided the *sboA* core peptide into three regions: the donor region (AA 1–13), loop region (AA 14–21), and acceptor region (AA 22–35) which contains acceptor residues for thioether bridges at positions a1, a7, and a10 (Figure 4). First, di- or tripeptides were introduced at two different loop positions and the well-known integrin binding RGD motif was chosen (Figure 5A).<sup>[16]</sup>

Resulting MALDI data showed that in all four variants three thioether bridges were formed, albeit with varying amounts of side products (Figure S13). It became apparent that insertions introduced closer to the *C*-terminal end of the loop region were preferably tolerated in terms of homogeneity of the peptide. Thus, *sboARG3* displayed a

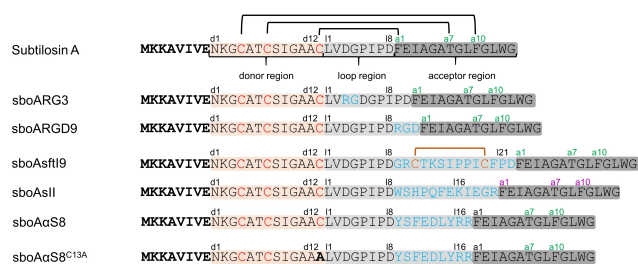


**Figure 4.** Schematic outline of loop insertion variants into the loop region of *sboA*. Identified acceptor positions are indicated in green (a1, a7 and a10). Proposed acceptor positions are highlighted in purple. Insertions are depicted in light blue and the C13 A mutation in *sboAaS8*<sup>C13A</sup> in bold. Proposed disulfide bridge is shown with an orange line. d1: first position of donor region, l1: first position of loop region, a1: first position of acceptor region.

higher amount of unmodified peptide compared to *sboARGD9* (Figure 5B). Additionally, the constructs showed presence of a sulfoxide derivative, probably at the *N*-terminal methionine (Figure S13).<sup>[17]</sup> MS/MS patterns of *sboARG3* and *sboARGD9* revealed the *sboA* wildtype connectivity, further providing evidence of a regioselective bridging activity of AlbA (Figure 5C, Figure S14 & S15).

To assess, whether a grafting strategy for longer loops could be employed in *sboA*, we further analyzed the tolerance of AlbA to the insertion of larger amino acid sequences into the loop region (Figure 5A). We considered the sequence of sunflower trypsin inhibitor I (SFTI) to be perfectly suited for this purpose for two reasons. First, natural SFTI, though being with its 14 amino acid residues a rather large fragment in terms of *sboA* peptide engineering, represents a disulfide-stabilized cyclic  $\beta$ -sheet.<sup>[18]</sup> This preorganized structure which has been reported to maintain its architecture also without head-to-tail cyclization motif and truncated, was supposed to be beneficial for the introduction of post-translational modifications into *sboA*. Second, natural SFTI contains two cysteine residues,<sup>[18,19]</sup> and therefore it was interesting to learn, whether AlbA would use these thiols for thioether bridge formation. To analyze the regiospecific tolerance of AlbA, the sequence of SFTI was introduced at different positions of the *sboA* loop (Figure 5A). Unsurprisingly, the *C*-terminal flexibility of AlbA was confirmed. The more remote the sequence from the *N*-terminus was, the more pronounced was the modification (Figure 5D, Figure S16, for overview see Table 1). While *sboAsfI9* showed three thioether cross links and one additional disulfide bridge, *sboAsfI5* showed a mixture of none, once and thrice modified fractions (Figure 5D). None of the constructs containing insertions in the proximity to the *N*-terminal part of the loop were modified by AlbA. Subsequent MS/MS analysis of *sboAsfI9* disclosed the *sboA* wildtype connectivity (acceptors a1, a7 and a10) (Figure 4, Figure S17). The disulfide was presumably formed between the two Cys residues of the SFTI sequence (Figure 4).

These results showed the ability of AlbA to catalyze thioether formation in *sboA* even when larger amino acid sequences are introduced at the end of the loop (19

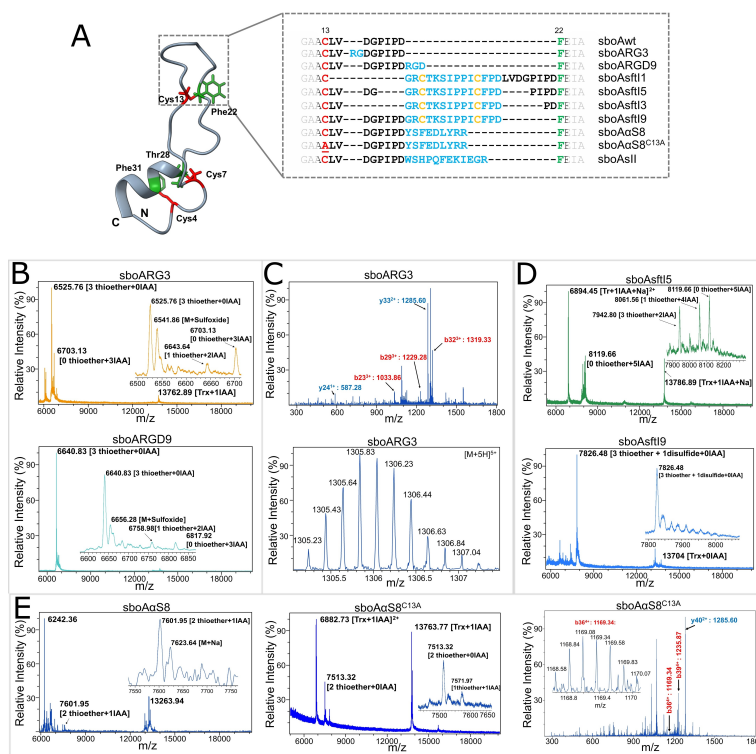


**Figure 5.** Tolerance of Alba to insertions in the loop of sbOA. A) Insertions of amino acid sequences into the loop of sbOA at different positions. Red: Cys involved in thioether modification, green: acceptor amino acid, blue: insertions, underlined: substitution yellow: involved in a disulfide bridge. B) MALDI results of small amino acid insertions. *SboARG3* and *sboARGD9* show full modification, however, *sboARG3* has a higher amount of unmodified peptide fraction. C) MS/MS results for *sboARG3* with respective b and y fragments. Lower panel shows  $[M+5H]^{5+}$  ion target in MS/MS. D) MALDI results of SFTI insertions. *SboAsf19* shows three thioethers and one disulfide bridge. E) MALDI results of *sboAaS8* (left panel) and *sboAaS8<sup>C13A</sup>* (middle panel) as well as MS/MS spectrum of *sboAaS8<sup>C13A</sup>* (right panel).

position). We further tested, whether this “19” position can be targeted as a versatile site for the implementation of other sequences to endow sactipeptides with alternative functions. Therefore, we introduced two additional amino acid sequences at the “19” position (Figure 4, Figure S18). These sequences varied in their length and structural preassembly. Alongside the linear 9-mer anti-idiotype tumor B-cell binding peptide S8,<sup>[20]</sup> a 12-mer sequence including the Strep-tag II peptide that binds engineered streptavidin was introduced at the 19 position.<sup>[21]</sup> Unexpectedly, for the 9-mer S8 peptide in *sboAaS8* only two thioether bridges were identified at the acceptor positions a7 and a10, further providing evidence of a regioselective bridging activity of Alba as the previous works indicated (Figure 4, Figure 5E & Figure S18).<sup>[4h,10]</sup> By replacing the Cys residue at position d13 by Ala we could demonstrate that indeed the formation of the sactionine between d13 and a1 was hampered by the introduced S8 sequence (Figure 5A & E, Figure S19). The reason for this might be the rather stringent and inflexible conformation of the loop not allowing the introduction of longer linear sequences. In contrast, introduction of the 12-mer sequence containing the Strep-tag II resulted in the formation of three sactionines in the corresponding construct (*sboAsII*, Figure 4 & Figure S18). Interestingly, Strep-tag II has a hairpin-like secondary structure even without covalent stabilization which also may contribute to the

appropriate relative orientation of residues involved in thioether bridge formation.<sup>[22]</sup> Hence, it is tempting to speculate that the peptide sequence to be inserted in the loop for engineering purposes may require some sort of structural preorganization to reach higher number of thioether bonds.

#### Streptavidin binding activity of grafted sbOA

The Strep-tag II sequence is known to bind the streptavidin variant Strep-Tactin in the nanomolar range.<sup>[21]</sup> To investigate binding of that peptide upon insertion into the sbOA framework, the C-terminal Strep-tag II was removed and the corresponding protein *sboAsII2-Trx* (Figure 6) was produced as already mentioned under semi-anaerobic conditions and pre-purified via IMAC (Figure 6, See Supporting Information for procedure). After removal of co-purified Alba, the protein solution was then applied to a Strep-Tactin column, where it was retained (Figure 6). This indicated a specific binding of the construct of interest to the Strep-Tactin resin. To verify that the bound construct was thioether bridged, the eluted fusion protein was incubated with TEV protease to cleave off the fusion partner and the sample was analyzed by MALDI-TOF-MS, revealing the presence of three thioether bridges as none of the Cys

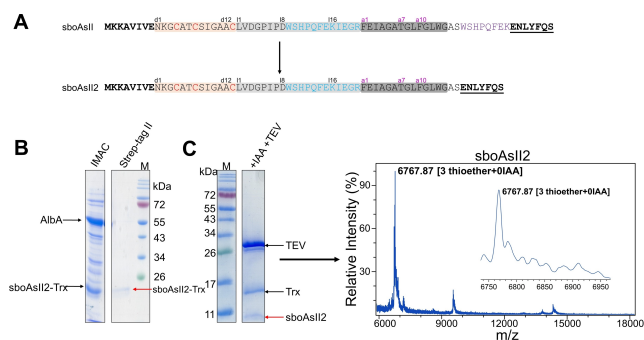


**Figure 6.** Strep-Tactin binding activity of *sboAsII2-Trx*. A) Design of *sboAsII2* without the C-terminal Strep-tag II sequence used for affinity purification of all sactipeptide constructs. B) Reducing SDS-PAGE of pooled IMAC fractions of *sboAsII2-Trx* (left) and elution fraction after Strep-Tactin binding (right). C) left: Reducing SDS-PAGE of TEV cleaved construct. Peptide of interest is marked with a red arrow. Right: MALDI-TOF-MS result of TEV cleaved sample after elution from the Strep-Tactin column showing the presence of three thioether bridges.

residues was labelled with IAA (Figure S20). This result showed that the internal Strep-tag II sequence conferred thrice thioether modified *sboA* with a novel protein pocket binding activity.

## Conclusion

In this present work, we analyzed the substrate promiscuity of the sactisynthase AlbA aimed at expanding the scope of its application to the engineering of sactipeptides—a promising though rather exotic class of sulfide-rich miniproteins. We demonstrated the limited ability of AlbA to modify non-native sactipeptides with a significantly decreased efficiency regarding the number of introduced thioethers when the *sboA* leader peptide replaced their respective leader sequence. Moreover, AlbA was able to access *sboA* hybrid peptides in which the *N*-terminal part consisted of *sboA* and the *C*-terminal part consisted of a non-native sactipeptide, and catalyzed the formation of thioether bridges in these constructs. These results corroborate the notion that sactipeptides can be engineered for biotechnological applications.<sup>[12]</sup> However, the number of successfully formed thioether bridges varied (For overview see Table 1). Our data strongly suggest that not only the acceptor positions are critical but also the surrounding sequence environment plays a role for AlbA substrate tolerance.

By combining our data and results from literature we could further demonstrate that the *sboA* loop region is particularly amenable to insertions and modifications.<sup>[4b,7c]</sup> Analysis of tolerance in the loop region of *sboA* revealed that both smaller and larger insertions were tolerated by AlbA to form thioether bridges. However, it became evident that larger insertions were only tolerated at the *C*-terminal part of the loop (I9 position). Notably, when a linear peptide of the length up to nine residues was introduced, formation of only two thioether bonds was observed and a mutagenesis analysis revealed that acceptor position a1, which is closest

to the loop insertion, is no longer recognized by AlbA. Replacement of Cys at the corresponding d13 position resulted in twice-modified product and we were pleased to see that the production yield improved significantly.

Since sactipeptides have a redox-stable rigid structure due to the presence of thioether bridges flanking an exposed loop region, they may become highly attractive scaffolds for the development of novel peptide-based therapeutics. Recently, the first in-human safety study of a lanthipeptide based GPCR agonist was reported, demonstrating the great potential of RiPPs possessing a thioether bridge in medicine.<sup>[23]</sup> While functionalization by loop grafting in lanthipeptides and cystine-knot peptides is a well-established strategy,<sup>[11a,23,24]</sup> usage of the sactipeptide scaffold for functionalization was lagging behind due to insufficient knowledge of loop tolerance and recombinant peptide synthesis strategies. In our proof-of-principle study, we demonstrated that functionalization and tailoring of sactipeptides is possible. We anticipate this strategy of inserting larger amino acid sequences into the loop region to be also suitable for other sactipeptides, given the corresponding sactisynthase tolerates these insertions. Further, this strategy could accelerate the development of a high throughput screening (HTS) platform for the directed evolution of sactipeptides as it has been done for other RiPPs.<sup>[11b,25]</sup>

Taken together, in this work we extended our knowledge about sactipeptides and sactisynthases; however, it further confronted us with questions to be addressed in future research. Our understanding of enzyme-driven thioether bridge formation in sactipeptides still lacks in-depth knowledge and needs extended investigation, especially concerning the introduction of modifications into non-native sactipeptides by sactisynthases.

## Acknowledgements

This work was supported by the German Research Foundation (DFG) through grant KO1390/13-1 (SPP2002). The authors want to thank the mass spectrometry core facility team of the Chemistry Department (TU Darmstadt) for measurements of the MALDI spectra and the German Research Foundation (DFG) through grant no INST 163/445-1 FUGG (MALDI MS). Open Access funding enabled and organized by Projekt DEAL.

## Conflict of Interest

The authors declare no conflict of interest.

## Data Availability Statement

The data that support the findings of this study are available from the corresponding author upon reasonable request.

**Keywords:** Bioengineering · Mini-proteins · RiPPs · Sactipeptides · Sactisynthases

- [1] a) O. Avrutina, *Adv. Exp. Med. Biol.* **2016**, *917*, 121–144; b) B. G. Lui, N. Salomon, J. Wustehube-Lausch, M. Daneschdar, H. U. Schmoldt, O. Tureci, U. Sahin, *Nat. Commun.* **2020**, *11*, 295.
- [2] a) J. R. Kintzing, J. R. Cochran, *Curr. Opin. Chem. Biol.* **2016**, *34*, 143–150; b) S. J. Moore, M. G. Hayden Gephart, J. M. Bergen, Y. S. Su, H. Rayburn, M. P. Scott, J. R. Cochran, *Proc. Natl. Acad. Sci. USA* **2013**, *110*, 14598–14603.
- [3] L. Cao, I. Goreschnik, B. Coventry, J. B. Case, L. Miller, L. Kozodoy, R. E. Chen, L. Carter, A. C. Walls, Y. J. Park, E. M. Strauch, L. Stewart, M. S. Diamond, D. Veessler, D. Baker, *Science* **2020**, *370*, 426–431.
- [4] a) K. Babasaki, T. Takao, Y. Shimonishi, K. Kurahashi, *J. Biochem.* **1985**, *98*, 585–603; b) K. E. Kawulka, T. Sprules, C. M. Diaper, R. M. Whittal, R. T. McKay, P. Mercier, P. Zuber, J. C. Vederas, *Biochemistry* **2004**, *43*, 3385–3395; c) H. Lee, J. J. Churey, R. W. Worobo, *FEMS Microbiol. Lett.* **2009**, *299*, 205–213; d) C. S. Sit, M. J. van Belkum, R. T. McKay, R. W. Worobo, J. C. Vederas, *Angew. Chem. Int. Ed.* **2011**, *50*, 8718–8721; *Angew. Chem.* **2011**, *123*, 8877–8880; e) M. C. Rea, C. S. Sit, E. Clayton, P. M. O'Connor, R. M. Whittal, J. Zheng, J. C. Vederas, R. P. Ross, C. Hill, *Proc. Natl. Acad. Sci. USA* **2010**, *107*, 9352–9357; f) C. Balty, A. Guillot, L. Fradale, C. Brewee, M. Boulay, X. Kubiak, A. Benjdia, O. Berteau, *J. Biol. Chem.* **2019**, *294*, 14512–14525; g) A. F. S. Duarte, H. Ceotto-Vigoder, E. S. Barrias, T. Souto-Padron, I. F. Nes, M. Bastos, *Int. J. Antimicrob. Agents* **2018**, *51*, 349–356; h) P. M. Himes, S. E. Allen, S. Hwang, A. A. Bowers, *ACS Chem. Biol.* **2016**, *11*, 1737–1744; i) G. A. Hudson, B. J. Burkhart, A. J. DiCaprio, C. J. Schwalen, B. Kille, T. V. Pogorelov, D. A. Mitchell, *J. Am. Chem. Soc.* **2019**, *141*, 8228–8238; j) L. Flühe, O. Burghaus, B. M. Wieckowski, T. W. Giessen, U. Linne, M. A. Marahiel, *J. Am. Chem. Soc.* **2013**, *135*, 959–962; k) C. S. Sit, R. T. McKay, C. Hill, R. P. Ross, J. C. Vederas, *J. Am. Chem. Soc.* **2011**, *133*, 7680–7683.
- [5] a) Y. Chen, J. Wang, G. Li, Y. Yang, W. Ding, *Front. Chem.* **2021**, *9*, 595991; b) A. Caruso, M. R. Seyedsayamdost, *J. Org. Chem.* **2021**, *86*, 11284–11289.
- [6] T. Mo, X. Ji, W. Yuan, D. Mandalapu, F. Wang, Y. Zhong, F. Li, Q. Chen, W. Ding, Z. Deng, S. Yu, Q. Zhang, *Angew. Chem. Int. Ed.* **2019**, *58*, 18793–18797; *Angew. Chem.* **2019**, *131*, 18969–18973.
- [7] a) A. Benjdia, C. Balty, O. Berteau, *Front. Chem.* **2017**, *5*, 87; b) N. Mahanta, G. A. Hudson, D. A. Mitchell, *Biochemistry* **2017**, *56*, 5229–5244; c) L. Flühe, T. A. Knappe, M. J. Gattner, A. Schafer, O. Burghaus, U. Linne, M. A. Marahiel, *Nat. Chem. Biol.* **2012**, *8*, 350–357.
- [8] T. L. Grove, P. M. Himes, S. Hwang, H. Yumerefendi, J. B. Bonanno, B. Kuhlman, S. C. Almo, A. A. Bowers, *J. Am. Chem. Soc.* **2017**, *139*, 11734–11744.
- [9] C. E. Shelburne, F. Y. An, V. Dholpe, A. Ramamoorthy, D. E. Lopatin, M. S. Lantz, *J. Antimicrob. Chemother.* **2007**, *59*, 297–300.
- [10] A. Benjdia, A. Guillot, B. Lefranc, H. Vaudry, J. Leprince, O. Berteau, *Chem. Commun.* **2016**, *52*, 6249–6252.
- [11] a) J. D. Hegemann, S. C. Bobeica, M. C. Walker, I. R. Bothwell, W. A. van der Donk, *ACS Synth. Biol.* **2019**, *8*, 1204–1214; b) J. H. Urban, M. A. Moosmeier, T. Aumüller, M. Thein, T. Bosma, R. Rink, K. Groth, M. Zully, K. Siegers, K. Tissot, G. N. Moll, J. Prassler, *Nat. Commun.* **2017**, *8*, 1500; c) J. D. Hegemann, R. D. Süßmuth, *ChemBioChem* **2021**, *22*, 3169–3172.
- [12] B. J. Burkhart, N. Kakkar, G. A. Hudson, W. A. van der Donk, D. A. Mitchell, *ACS Cent. Sci.* **2017**, *3*, 629–638.
- [13] N. A. Bruender, V. Bandarian, *Biochemistry* **2016**, *55*, 4131–4134.
- [14] S. Chiumento, C. Roblin, S. Kieffer-Jaquinod, S. Tachon, C. Lepretre, C. Basset, D. Adityarini, H. Olleik, C. Nicoletti, O. Bornet, O. Iranzo, M. Maresca, R. Hardre, M. Fons, T. Giardina, E. Devillard, F. Guerlesquin, Y. Coute, M. Atta, J. Perrier, M. Lafond, V. Duarte, *Sci. Adv.* **2019**, *5*, eaaw9969.
- [15] C. Balty, A. Guillot, L. Fradale, C. Brewee, B. Lefranc, C. Herrero, C. Sandstrom, J. Leprince, O. Berteau, A. Benjdia, *J. Biol. Chem.* **2020**, *295*, 16665–16677.
- [16] H. Schneider, S. Englert, A. Macarron Palacios, J. A. Lerma Romero, A. Ali, O. Avrutina, H. Kolmar, *Front. Chem.* **2021**, *9*, 693097.
- [17] P. T. Wingfield, *Curr. Protoc. Protein Sci.* **2017**, *88*, 6.14.1–6.14.3.
- [18] H. Fittler, O. Avrutina, M. Empting, H. Kolmar, *J. Pept. Sci.* **2014**, *20*, 415–420.
- [19] D. Debowski, R. Lukajtis, M. Filipowicz, P. Strzelecka, M. Wysocka, A. Legowska, A. Lesner, K. Rolka, *Biopolymers* **2013**, *100*, 154–159.
- [20] J. Torchia, K. Weiskopf, R. Levy, *Proc. Natl. Acad. Sci. USA* **2016**, *113*, 5376–5381.
- [21] T. G. M. Schmidt, A. Eichinger, M. Schneider, L. Bonet, U. Carl, D. Karthaus, I. Theobald, A. Skerra, *J. Mol. Biol.* **2021**, *433*, 166893.
- [22] a) T. G. Schmidt, J. Koepke, R. Frank, A. Skerra, *J. Mol. Biol.* **1996**, *255*, 753–766; b) S. Voss, A. Skerra, *Protein Eng.* **1997**, *10*, 975–982.
- [23] P. Namsolleck, A. Richardson, G. N. Moll, A. Mescheder, *Peptides* **2021**, *136*, 170468.
- [24] C. P. Sommerhoff, O. Avrutina, H. U. Schmoldt, D. Gabrijelcic-Geiger, U. Diederichsen, H. Kolmar, *J. Mol. Biol.* **2010**, *395*, 167–175.
- [25] a) T. Bosma, A. Kuipers, E. Bulten, L. de Vries, R. Rink, G. N. Moll, *Appl. Environ. Microbiol.* **2011**, *77*, 6794–6801; b) E. Reyna-Gonzalez, B. Schmid, D. Petras, R. D. Süßmuth, E. Dittmann, *Angew. Chem. Int. Ed.* **2016**, *55*, 9398–9401; *Angew. Chem.* **2016**, *128*, 9544–9547.

Manuscript received: July 24, 2022

Accepted manuscript online: September 1, 2022

Version of record online: October 12, 2022